# Supporting Information for "Micromechanics of sheared granular layers activated by fluid pressurization"

Hien Nho Gia Nguyen[1], Luc Scholtès[1,2], Yves Guglielmi[3], Frédéric Victor

Donzé[4], Zady Ouraga[5], Mountaka Souley[5]

[1]Université de Lorraine, CNRS, GeoRessources, Nancy, France

[2]Université Clermont Auvergne, CNRS, IRD, OPGC, Laboratoire Magmas et Volcans, Clermont-Ferrand, France

[3]Lawrence Berkeley National Laboratory, Energy Geosciences Division, Berkeley, CA, USA

[4]Université Grenoble-Alpes, CNRS, ISTerre, Grenoble, France

[5]Ineris, Verneuil-en-Halatte, France

## Contents of this file

―――――

March 8, 2021, 5:52pm

## 1. DEM-PFV formulations

The numerical sample consists of smooth spherical particles. The DEM module handles the solid phase while the PFV module handles the fluid phase.[1] The DEM is based on a Lagrangian approach where each particle is identified by its own mass, size and moment of inertia. The computation scheme consists in integrating Newton's second law so as to determine particles motion and interactions one with another. The DEM model is a 3D implementation in the open source code YADE-DEM where interparticle contacts are modeled by linear elastic relationships between forces and interparticle displacements, associated with a slip Coulomb model. The contact laws governing the interactions are defined from 3 parameters including the normal stiffness coefficient $k_n$, the tangent stiffness coefficient $k_t$ and the microscopic friction coefficient $\mu_p$ (Cundall & Strack, 1979). The inter-particle contact behavior have two components: (1) the normal contact is governed by an elastic force-displacement relation $\Delta F_n = k_n \Delta \delta_c \geq 0$ where $\delta_c$ is the overlapping between two particles in contact; (2) the tangent force is incrementally computed at each numerical time step as $\Delta F_t = k_t \Delta u_t$ and $|F_t| \leq F_n \tan \mu_p$. The parameters for the contact laws are given in Table S1. The numerical sample consists of 12,000 spherical particles with a uniform size distribution whose diameters vary between $0.066 \, \mathrm{mm}$ and $0.133 \, \mathrm{mm}$ with the density of $2600 \, \mathrm{kg/m^3}$. The microscopic friction coefficient $\mu_p$ is 0.52.

For the fluid coupling, the PFV module is able to describe the compressible flow at the particle scale in the viscous regime. A partition of the pore space is obtained by constructing the regular triangulation of the packing. The elementary objects emerging from this procedure are tetrahedrons whose vertices are defined by the centers of gravity

of the particles. The space limited by this structure is known as the pore space. For the sake of simplicity, the information in this document is a summary extracted from (Scholtès et al., 2015). More details of the PFV formulation can be found in (Chareyre et al., 2012).

Let us define $\Omega_i$ the portion of the pore $i$ occupied by the fluid (Figure S1). Integrating the continuity equation in $\Omega_i$ gives:

$$\int_{\Omega_i} \frac{\partial \rho_f}{\partial t} dV = -\int_{\Omega_i} \nabla \cdot (\rho_f \mathbf{v}) \, dV \tag{1}$$

where $\rho_f$ is the fluid density and $\mathbf{v}$ is the fluid velocity. Applying the divergence theorem leads Eq. (1) to

$$\int_{\Omega_i} \frac{\partial \rho_f}{\partial t} dV = -\int_{\partial \Omega_i} \rho_f \mathbf{v} \cdot \mathbf{n} dS \tag{2}$$

with $\mathbf{n}$ the outward pointing unit vector normal to $\partial \Omega_i$. As the vertices of the elements follow the motion of the particles, the element is deforming at a certain rate. Introducing $\mathbf{u}$ as the velocity of the contour $\partial \Omega_i$, Eq. (2) can be written as:

$$\int_{\Omega_i} \frac{\partial \rho_f}{\partial t} dV = -\int_{\partial \Omega_i} \rho_f (\mathbf{v} - \mathbf{u}) \cdot \mathbf{n} dS - \int_{\partial \Omega_i} \rho_f \mathbf{u} \cdot \mathbf{n} dS \tag{3}$$

The bulk modulus $K_f$ relates the time derivatives of $\rho_f$ and $P_i$ as

$$K_f = \rho_f \frac{\partial P_i}{\partial \rho_f}, \tag{4}$$

for a compressible fluid.

March 8, 2021, 5:52pm

For saturated media (degree of saturation $S_r = 1$), $K_f$ is equal to the fluid bulk modulus (e.g. water $K_w = 2.2 \times 10^9$ Pa). If air phase is available in the fluid ($0.9 < S_r < 1$), $K_f$ depends on the gaz content in the fluid mixture:

$$K_f = \frac{1}{\dfrac{S_r}{K_w} + \dfrac{1 - S_r}{K_a}} \tag{5}$$

assuming the air distribution within fluid is uniform in all pores, with $K_a$ the bulk modulus of air.

Considering Eq. (4) and neglecting the spatial fluctuation of $\rho_f$ in the vicinity of the domain (small Mach number), Eq. (3) thus becomes

$$\int_{\Omega_i} \frac{1}{K_f} \frac{\partial P_i}{\partial t} dV = -\sum_{j=1}^{4} \int_{S_{ij}^f} (\mathbf{v} - \mathbf{u}) \cdot \mathbf{n} dS - \dot{V}_{p,i} \tag{6}$$

where $\dot{V}_{p,i}$ is the time derivative of the pore volume and $S_{ij}^f$ is the intersection of the triangular surface with the fluid domain along each side of the tetrahedron.

The fluxes integrals appearing on the right-hand side of Eq(6) can be linked to the pressure jump between two pores $i$ and $j$ so that the equation becomes

$$\dot{P}_i = -\frac{K_f}{V_{f,i}} \left[ \dot{V}_{p,i} + \sum_{j=1}^{4} k_{ij} (P_i - P_j) \right] \tag{7}$$

with $k_{ij}$ the conductivity of the thoat between $i$ and $j$, $k_{ij}$ being computed as a function of the thoat geometry through a generalized Poiseuille's law.

A finite difference discretization of Eq. (7) using a backward Euler scheme for the evaluation of $\dot{P}_i$ gives

$$\sum_{j=1}^{4} k_{ij} P_j^t - \left( \zeta_i + \sum_{j=1}^{4} k_{ij} \right) P_i^t = \dot{V}_{p,i}^{t-1/2} - \zeta_i P_i^{t-1}, \quad \text{with} \quad \zeta_i = \frac{V_{f,i}}{K_{\mathrm{f}} \Delta t} \tag{8}$$

where the time-centered evaluation of $\dot{V}_{p,i}^{t-1/2}$ is obtained from mid-step velocities of the particles. An implicit scheme is obtained by considering Eq. (8) for all pores at a given time. The associated linear system has to be solved as each time-step of the simulation, linking the pressure field $P^t$ to the deformation rate of the pore space.

In turn, the force exerted by the fluid on each particle $p$ can be deduced using the same expressions as for an incompressible fluid. It is the sum of three terms which are contour integrals of the hydrostatic pressure $\rho_{\mathrm{f}} g z$ (buoyancy), of the piezometric pressure $P$ and the viscous shear stress $\boldsymbol{\tau}$, respectively:

$$\mathbf{F}^p = \int_{\Gamma_p} \rho_{\mathrm{f}} g z \mathbf{n} \mathrm{d}S + \int_{\Gamma_p} P \mathbf{n} \mathrm{d}S + \int_{\Gamma_p} \tau \mathbf{n} \mathrm{d}S = \mathbf{F}^{B,p} + \mathbf{F}^{P,p} + \mathbf{F}^{V,p}, \tag{9}$$

$\Gamma_p$ is the solid surface of the particle $p$. These forces are determined for time $t$ and integrated into the conventional explicit time-stepping algorithm of the DEM by summing them together with the contact forces. This sequence of equations (8) and (9) defines a semi-implicit integration scheme.

## 2. Analysis methods

### 2.1. Extracting sub-sample

While the numerical sample is three dimensional and it has periodic boundaries on the horizontal directions, a vertical slide with thickness of about 15 particles is sufficient for the analysis. This sub-sampling method allows the efficiency of the analysis while maintain the clearance of data visualization by projecting 3D data point on a 2D diagram.

## 2.2. Particle rotation calculation

The accumulated rotation of the particle is calculated from the snapshots of the sample between two stages: the current selected stage versus the initial stage where the fluid injection starts (P $=$ 0 MPa).

## 2.3. Contact force network

The contact force network is a set of particle-particle interactions visualized based on the position of the grains in contact and the intensity of their local contact force. At a selected stage, normal contact forces of all interaction can be computed as mentioned in Section 1. The line segments represent the vector branch connecting two particles in contact. For the normalization, the max and min of normal contact forces from all three stages are taken into account. Then, the normalization is based on these max and min values, enabling a consistent comparison method.

## 2.4. Sliding contact detection

For a particle-particle interaction, when the computed tangent force $F_t$ exceeds the threshold $F_n \tan \mu_p$, the contact is defined as a 'sliding contact'. The position of a sliding contact is the midpoint of two involved particles. It worths noting that it is expected to have high amount of sliding contacts at the boundaries (top and bottom plates) because of the shear control is governed by the plate movement. Hence, in order to focus better on what happens within the sample, especially around the shear band, the sliding contacts near the boundaries are not displayed.

**References**

March 8, 2021, 5:52pm

Chareyre, B., Cortis, A., Catalano, E., & Barthélemy, E. (2012). Pore-Scale Modeling of Viscous Flow and Induced Forces in Dense Sphere Packings. *Transport in Porous Media*, *92*(2), 473-493. doi: 10.1007/s11242-011-9915-6

Cundall, P. A., & Strack, O. D. L. (1979). A discrete numerical model for granular assemblies. *Géotechnique*, *29*(1), 47-65. doi: 10.1680/geot.1979.29.1.47

Scholtès, L., Chareyre, B., Michallet, H., Catalano, E., & Marzougui, D. (2015). Modeling wave-induced pore pressure and effective stress in a granular seabed. *Continuum Mechanics and Thermodynamics*, *27*(1), 305-323. doi: 10.1007/s00161-014-0377-2

**Notes**

1. DEM: discrete elements method, PFV: pore-scale finite volume

March 8, 2021, 5:52pm

**Table S1.** Model properties

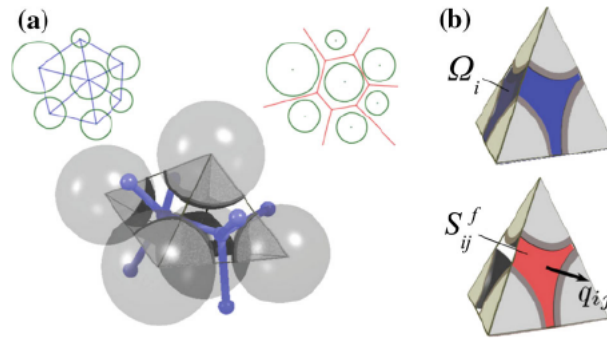| Particles and contacts | value | Bulk (steady-state) | value |
|---|---|---|---|
| Particle diameter $D_p$ | $0.1 \pm 0.033\,\mathrm{mm}$ | Porosity $n$ | 0.438 |
| Particle density $\rho_p$ | $2{,}600\,\mathrm{kg/m^3}$ | Permeability $k_x = k_z = 2k_y$ | $2.4 \cdot 10^{-11}\,\mathrm{m^2}$ |
| Normal stiffness $\frac{k_n}{D_p}$ | $1\,\mathrm{GPa}$ | Normal stiffness $K_n$ | $20.9\,\mathrm{MPa{\cdot}m}$ |
| Shear stiffness $\frac{k_s}{D_p}$ | $0.25\,\mathrm{GPa}$ | Shear stiffness $K_s$ | $5\,\mathrm{MPa{\cdot}m}$ |
| Friction coefficient $\mu_p$ | 0.52 | Friction coefficient $\mu$ | $0.38 \pm 0.01$ |



**Figure S1.** (a) Regular triangulation and its dual Voronoi's graph in two dimensional and in three dimensional. (b) Elementary fluid domain (tetrahedron) in triangulated sphere assembly.